On the Small Crack Fracture Mechanics.

Ståhle, P.

Published in:
International Journal of Fracture

1983

Document Version:
Publisher's PDF, also known as Version of record

Citation for published version (APA):
Ståhle, P. (1983). On the Small Crack Fracture Mechanics. *International Journal of Fracture*, *22*(3), 203-216.

Total number of authors:
1

Int. Journ. of Fracture 22 (1983) 203–216

On the small crack fracture mechanics

P. STÅHLE

Division of Solid Mechanics, Lund Institute of Technology, Lund, Sweden

(Received July 6, 1981; in revised form June 12, 1982)

ABSTRACT

The limit of validity of linear fracture mechanics is specified by the minimum allowable crack length through an ASTM convention. Extension into the non-linear region ought to imply an extension towards smaller allowable cracks. In order to elucidate the question "How short is the smallest crack that fits the methods of fracture mechanics, and how do shorter cracks than that behave?" a pilot investigation is carried out. The process region is modelled as a Barenblatt line region and plastic flow off-side the process region is neglected. Results show that instability occurs before the process region is fully developed (as at large cracks) if the crack is short. This implies large deviations from the large crack fracture mechanics if the crack is very small. Even cracks of infinitesimal length are included in the study.

1. Introduction

The validity of the linear fracture mechanics was clearly specified quite early by the ASTM convention [1]

$$a \geqslant 2.5(K_{Ic}/\sigma_y)^2$$

where a is a significant crack length parameter, K_{Ic} the fracture toughness and σ_y the yield stress. The role of linear fracture mechanics is, however, very limited in engineering practice. Very often cracks much smaller than those for which linear fracture mechanics is applicable are detected. However, there does not seem to be a reliable condition for the validity of non-linear fracture mechanics, for instance of the variety that uses J-integral methods. The present work is intended as a study of small cracks, extended towards vanishing crack lengths. It is a pilot study, only, because the total dissipative region is assumed to consist of a Barenblatt type process region [2]. This implies, among other things, that no stable crack growth takes place (even though the edge of the process region moves stably under controlled conditions). However, it is believed that the investigation may help to shed some light on the specific phenomena appearing in connection with very small cracks.

2. The model

A homogeneous elastic body containing a mode I crack with the length $2a_0$ and decohesive process regions with the length $(a - a_0)$, each, is considered (see Fig. 1). A stress σ_∞ is remotely applied under conditions of plane stress or strain. The fracture process takes place at the decohesive regions where the stress is decreasing at increasing displacement. These regions are supposed to grow symmetrically in the crack plane $y = 0$.

A simple model of the relationship between bonding force per unit area and discontinuous displacement, σ_{yy} *vs.* v, describes the mechanical properties of the process region (Fig. 2), and introduces a length quantity, that may serve as a scaling factor.

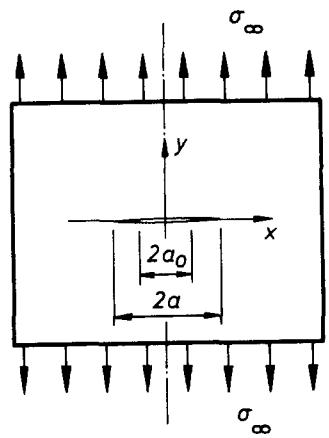

Figure 1. An infinite body with a crack, under plane stress or strain.

For a crack of length $2a_0$, the total length of the discontinuous zone, i.e. crack plus process regions, $2a$, is asked for. The solution is governed by the remotely applied stress σ_∞, and the material is described by the modulus of elasticity E, Poisson's ratio ν and a yield strength large enough in comparison with the maximum stress in the process region, σ_D, that plastic flow does not occur off-side the process region. During the process of loading, the length of the process region increases, giving larger and larger displacements at the crack tip until the limit displacement v^* is reached. The process region is then said to be fully developed since after this the tip of the region can only advance if the crack grows under the constraint $\sigma_{yy}(v > v^*) = 0$.

3. Analysis

The model corresponds to the following problem in the theory of elasticity: A linearly elastic semi-infinite body, occupying the upper half plane $y > 0$, is subject to the remote stress σ_∞ and the following boundary conditions on $y = 0$;

$$\begin{aligned} &\tau_{xy} = 0 \\ &\sigma_{yy} = 0 \qquad \text{for} \quad |x| < a_0, \\ &\sigma_{yy} = \sigma_{yy}(v) \quad \text{for} \quad a_0 < |x| < a, \\ &\text{and } v = 0 \qquad \text{for} \quad a < |x|. \end{aligned} \tag{1}$$

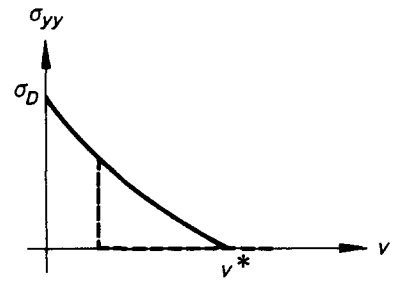

Figure 2. Decohesion stresses *vs.* discontinous displacements at the process region. The stresses can be zero at parts where $v < v^*$, if these formed the original slit from which the process region develops.

The Muskhelishvili [3] complex potentials $\Phi(z)$ and $\psi(z)$ are used, where $z = x + iy$. By defining $\Phi(z)$ as $\bar{\Phi}(z) + z\bar{\Phi}'(z) + \bar{\psi}(z)$ in $y < 0$, one may eliminate $\psi(z)$ and obtain

$$\sigma_{xx} + \sigma_{yy} = 2[\Phi(z) + \bar{\Phi}(\bar{z})] \tag{2}$$

$$\sigma_{yy} - i\tau_{xy} = \Phi(z) + \Phi(\bar{z}) + (z - \bar{z})\bar{\Phi}'(\bar{z}) \tag{3}$$

and

$$2\mu(u' + iv') = \kappa\Phi(z) - \Phi(\bar{z}) - (z - \bar{z})\bar{\Phi}'(\bar{z}) \tag{4}$$

where

$$\mu = E/[2(1 + \nu)] \text{ and } \kappa = \begin{cases} (3 - \nu)/(1 + \nu) & \text{in plane stress} \\ 3 - 4\nu & \text{in plane strain.} \end{cases}$$

Without loss of generality the plane strain case is chosen for inspection. Solutions for plane stress are obtained by replacing ν with $\nu/(1 + \nu)$ and E with $E(1 + 2\nu)/(1 + \nu)^2$.

Along the x-axis (3) and (4) will give, due to the symmetry of τ_{xy} and u with respect to the line $y = 0$,

$$\sigma_{yy} = \Phi_+ + \Phi_-$$

and

$$\partial v/\partial x = \frac{2(1 - \nu^2)}{iE}(\Phi_+ - \Phi_-) \tag{5}$$

where

$$\Phi_\pm(x) = \lim_{y \to 0} \Phi(x \pm iy) \quad y > 0.$$

Thus the boundary conditions can be written on the form

$$\Phi_+(t) + G(t)\Phi_-(t) = f(t)$$

where

$$G(t) = \begin{cases} 1 & \text{for } |t| < a \\ -1 & \text{for } a < |t| \end{cases}$$

and

$$f(t) = \begin{cases} \sigma_{yy}(t) & \text{for } a_0 < |t| < a \\ 0 & \text{for } |t| < a_0 \text{ and } a < |t|. \end{cases}$$

The solution (c.f. Muskhelishvili [3]) is

$$\Phi(z) = (i/\pi)z(z^2 - a^2)^{-1/2} \int_{a_0}^{a} \sigma_{yy}(t)(t^2 - a^2)^{1/2}(z^2 - t^2)^{-1}\, dt + (z^2 - a^2)^{-1/2}p(z) \tag{6}$$

where $p(z)$ can, on account of the symmetry and by letting $z \to \infty$ be identified with $\sigma_\infty z/2$. The assumption that the stresses should remain bounded everywhere and especially at $z = \pm a$ implies

$$\sigma_\infty = (2/\pi) \int_{a_0}^{a} \sigma_{yy}(t)(a^2 - t^2)^{-1/2}\, dt. \tag{7}$$

Letting $y \to 0$, (5), (6) and (7) give

$$\partial v/\partial x = \frac{4(1-\nu^2)}{\pi E} \cdot x(a^2 - x^2)^{-1/2} \int_{a_0}^{a} \sigma_{yy}(t)[(a^2 - t^2)^{1/2}(x^2 - t^2)^{-1} - \\ - (a^2 - t^2)^{-1/2}]\,dt. \tag{8}$$

It is easily checked that the boundedness of the stresses at the process region implies that it closes smoothly, that is $v \propto (a^2 - x^2)^{3/2}$ close to the tips of the process regions. After integration (8) reads

$$v(x) = \frac{2(1-\nu^2)}{\pi E} \int_{a_0}^{a} \sigma_{yy}(t)\{\ln[(a^2 - x^2)^{1/2} + (a^2 - t^2)^{1/2}] - \\ - \ln|(a^2 - x^2)^{1/2} - (a^2 - t^2)^{1/2}| - 2[(a^2 - x^2)/(a^2 - t^2)]^{1/2}\}\,dt. \tag{9}$$

In the model it was assumed that σ_{yy} is a given function of v. Knowledge of this function enables calculation of relations between σ_{yy} and x for the process region. Conversely, given a distribution with respect to x, the resulting σ_{yy} *vs.* v relationship can be calculated. Here, two choices for the σ_{yy} distribution at the process region are evaluated, one for a linear σ_{yy} *vs.* x relationship:

$$\text{model A:} \quad \sigma_{yy} = \sigma_D\left(1 - \frac{x-a}{a_0 - a} v_0/v^*\right) \tag{10}$$

where v_0 is the displacement at the crack tip, and one for a linear σ_{yy} *vs.* v relationship:

$$\text{model B:} \quad \sigma_{yy} = \sigma_D(1 - v(x)/v^*). \tag{11}$$

Model B certainly describes reality better than model A. A certain σ_{yy} *vs.* x relationship gives rise to different σ_{yy} *vs.* v relationships, depending upon which instant of the process region growth is selected for inspection. The reason why model A nevertheless is used depends upon its suitability for analytical treatment. Comparison between the two models will later be made.

Model A: $\sigma_{yy} = \sigma_{yy}(x, v_0)$

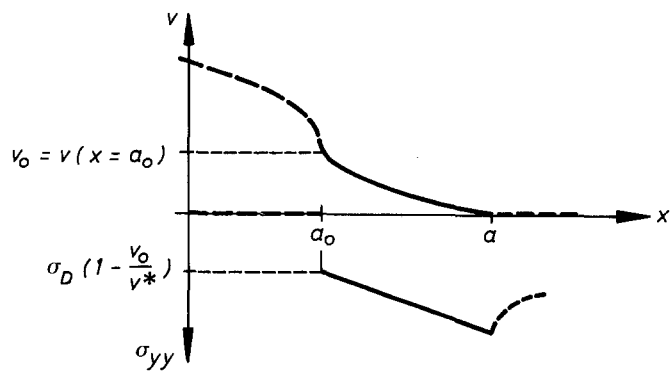

Figure 3. Displacement and stress distribution at the process region. The stresses are connected with the displacements through the relationship $\sigma_{yy}(a_0) = \sigma_D(1 - v_0/v^*)$.

The idea of model A is to fix two points of the resulting σ_{yy} *vs.* v relationship namely $\sigma_{yy} = \sigma_D$ at $x = a$ where the displacement is approaching zero and at the crack tip $x = a_0$ where the stress is supposed to assume the value $\sigma_D(1 - v_0/v^*)$ where v_0 is the displacement at this point (see Fig. 3). The integration of (9) and (7) is straight forward but cumbersome. The result is

$$v(x) = \frac{2(1-\nu^2)\sigma_D}{\pi E}\left\{\left[1 - \frac{a}{a-a_0}\cdot v_0/v^*\right]\cdot\left[a_0 \coth^{-1}\left(\left(\frac{a^2-a_0^2}{a^2-x^2}\right)^{1/2}\right) - \right.\right.$$
$$- x\coth^{-1}\left(\frac{x}{a_0}\cdot\left(\frac{a^2-a_0^2}{a^2-x^2}\right)^{1/2}\right) +$$
$$+ \frac{1}{a-a_0}\cdot(v_0/v^*)\left[\frac{a_0^2-x^2}{2}\coth^{-1}\left(\left(\frac{a^2-a_0^2}{a^2-x^2}\right)^{1/2}\right) + \right.$$
$$\left.\left. + (a-x^2)^{1/2}(a-a_0)^{1/2}\right]\right\} \tag{12}$$

$$\sigma_\infty = (2/\pi)\sigma_D\left\{\left[1 - \frac{a}{a-a_0}(v_0/v^*)\right]\cos^{-1}(a_0/a) + \right.$$
$$\left. + (v_0/v^*)[(a+a_0)/(a-a_0)]^{1/2}\right\}. \tag{13}$$

Note that $\coth^{-1} x = (1/2)\ln[(x+1)/(x-1)]$. The length of the process region $(a - a_0)$ is determined by the remote stress σ_∞. Here solutions are produced using a and a_0 as parameters in calculating σ_∞. To do this (12) is used to determine the crack tip displacement

$$v_0/v^* = \lim_{x\to a_0} v(x)/v^* = 2\beta\ln\beta/[1 + \beta + 2\beta\ln\beta/(1-\beta) - \alpha] \tag{14}$$

where two dimensionless quantities, $\beta = a_0/a$ and $\alpha = \pi E v^*/[2(1-\nu^2)\sigma_D a]$ are introduced. Thus a situation where the tip of the process region is advancing while the crack tip remains constant prevail when $v_0 < v^*$. After the limit $v_0 = v^*$ is reached a and a_0 are no longer independent but a_0 must be chosen to fulfil the condition $v_0 = v^*$, that is, when a is increasing, a_0 must increase too, to prevent v_0 from getting larger than v^*. In this case a_0 is found by putting $v_0/v^* = 1$ in (14), which leads to the expression

$$a_0 = \frac{\pi E v^*}{2(1-\nu^2)\sigma_D}\cdot\beta(1-\beta)/(1-\beta^2+2\beta^2\ln\beta). \tag{15}$$

Model B: $\sigma_{yy} = \sigma_{yy}(v)$

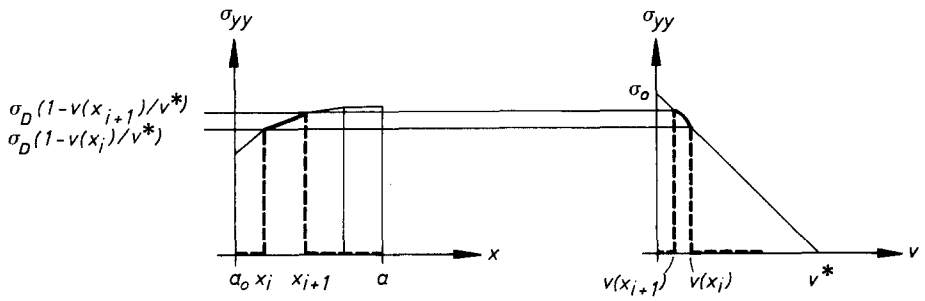

Figure 4. One of the N parts from which a complete process region is constructed. Stresses are linearly distributed with respect to x in each part but the magnitudes are chosen to give a linear σ_{yy} *vs.* v relationship.

For the second choice, model B, a numerical solution is obtained using (12). The interval between a_0 and a is divided into N parts of equal length in which the stresses are supposed to vary linearly with with respect to x. To begin with, a solution for a "process region" extending from a_i to a_{i+1} (see Fig. 4) is constructed. Putting

$$\sigma_{yy}(x) = \sigma_D\left[1 - \frac{a_{i+1}}{a_{i+1} - a_i}\cdot(v(a_i)/v^*) + \frac{a_i}{a_{i+1} - a_i}\cdot(v(a_{i+1})/v^*) + \right.$$
$$\left. + \left(\frac{1}{a_{i+1} - a_i}\cdot(v(a_i)/v^*) - \frac{1}{a_{i+1} - a_i}\cdot(v(a_{i+1})/v^*)\right)x\right]$$

for $a_i < x \leqslant a_{i+1}$, the displacements caused by this stress distribution can be calculated

$$v(x) = A(x)\cdot v(a_i) + B(x)\cdot v(a_{i+1}) + C(x)$$

where A, B and C are determined by calculating the integral in (9) after change of the interval a_i to a_{i+1}. Superposing such stress distributions to form a complete process region v becomes a function of x and a linear function of $v(a_i)$ where $i = 1, 2, 3 \ldots, N - 1$.

$$v(x) = D(x) + \sum_{i=0}^{N-1} E(x)\cdot v(a_i) \tag{16}$$

A system of N equations is obtained by letting x assume the values $a_0, a_1 \ldots a_{N-1}$. This can be written on a simpler form

$$V = D + E\cdot V$$

where $V = (v(a_0), v(a_1) \ldots v(a_{N-1}))^T$ and D and E are $N \times N$ matrixes. Now the displacements V are found to be

$$V = (I - E)^{-1}D$$

where I is the unit matrix. From these, the displacements throughout the process region are found using (16).

4. Result

With the models studied formation of process regions occurs at infinitesimally small load. With increasing load the process regions grow into the elastic material, replacing the linear elastic continuum with a linear σ_{yy} *vs.* x relationship (Fig. 5a) or a linear σ_{yy} *vs.* v relationship (Fig. 5b). In both cases the relation $\sigma_{yy} = \sigma_D(1 - v_0/v^*)$ is fulfilled at the crack tip. The consequence is that the stress discontinuity here, must drop as the process region penetrates into fresh material, since the crack tip displacement, as is seen from the analysis, is increasing monotonically. For a certain length of the process region the stress discontinuity vanishes, i.e. when $v = v^*$ at x = a_0. From here on, the crack expands with the subsidary condition that σ_{yy} must be zero behind the point where $v = v^*$. These situations, when the process region is fully developed are separately treated below and specify a well defined group of solutions where σ_∞ and a_0 are uniquely determined for every choice of σ_{yy} *vs.* v relationship.

During the formation of the process region, a remotely applied stress equilibrates the stresses σ_{yy} in the crack plane, $y = 0$. This remote stress is plotted *vs.* length of the discontinuous zone in Figs. 6a and 6b. Starting at (A) with a slit of length. $4\pi Ev^*/[(1 - \nu^2)\sigma_D]$, the process region expands under an increasing remote stress to (B). When the region

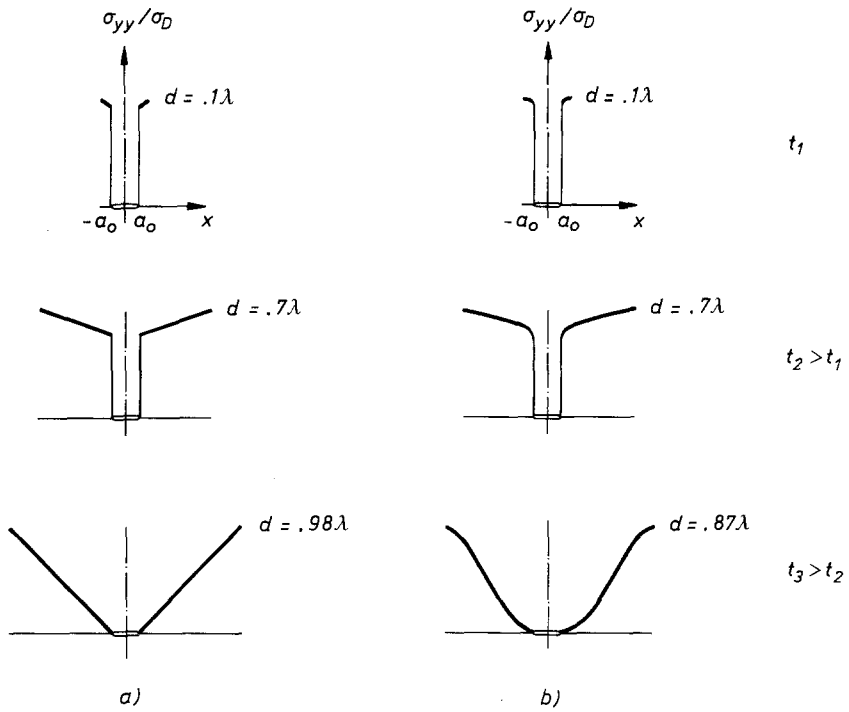

Figure 5. Development of the stresses at a process region, originating from a slit, upon loading. (a) corresponds to model A and (b) to model B. $d = a - a_0$ is the length of the process region and $\lambda = \pi E v^*/(2(1 - \nu^2)\sigma_D)$ is a length parameter.

expands further the remote stress decreases and finally the fully developed state of the process region is achieved at (*C*). While the state of the discontinuity has extended from a slit (*A*) to a crack with a fully developed process region at (*C*), the crack length, i.e. the length of the traction free surface, has remained constant. It is also observed from Fig. 6, that the crack cannot be held stably at equilibrium, under fixed load conditions, beyond the point (*B*). Nevertheless physical states past maximum load, where the discontinuous zone is enlarged under a decreasing remote stress, may be of practical interest considering the finite stiffness of engineering structures, under so called fixed grip conditions.

In the case of large slits, maximum load occurs immediately before the process region is fully developed (see Fig. 6 and appendix). So, no matter the length of the crack, no stable crack growth is found, only a stable growth of the process region, since instability always occurs before the process region is fully developed, i.e. before crack growth.

Analysing the load response of a body with an infinitesimally small crack, it is found that a process region with a constant cohesive stress is developed but when the zone length reaches a size of about $\pi E v^*/[2(1 - \nu^2)\sigma_D]$, it collapses and a crack is formed.

Fully developed process region. To analyse the growing crack one must find a pair a and a_0 such that $v = v^*$ at $x = a_0$. The procedure for model A is shortly, to find, for a fixed quotient $\beta = a_0/a$, the length of the crack, a_0, from (15). The analysis is uncomplicated and it is easily seen that all solutions are covered. The function $f(\beta) = \beta(1 - \beta)/(1 - \beta^2 + 2\beta^2 \ln \beta)$ (c.f. Eqn. (15)) is single-valued in the interval $0 < \beta < 1$ and by inspection one finds that $\beta \to 1$ implies $a_0 \to \infty$ and $\beta \to 0$ implies $a_0 \to 0$. The region lengths are shown in Fig. 7. The length

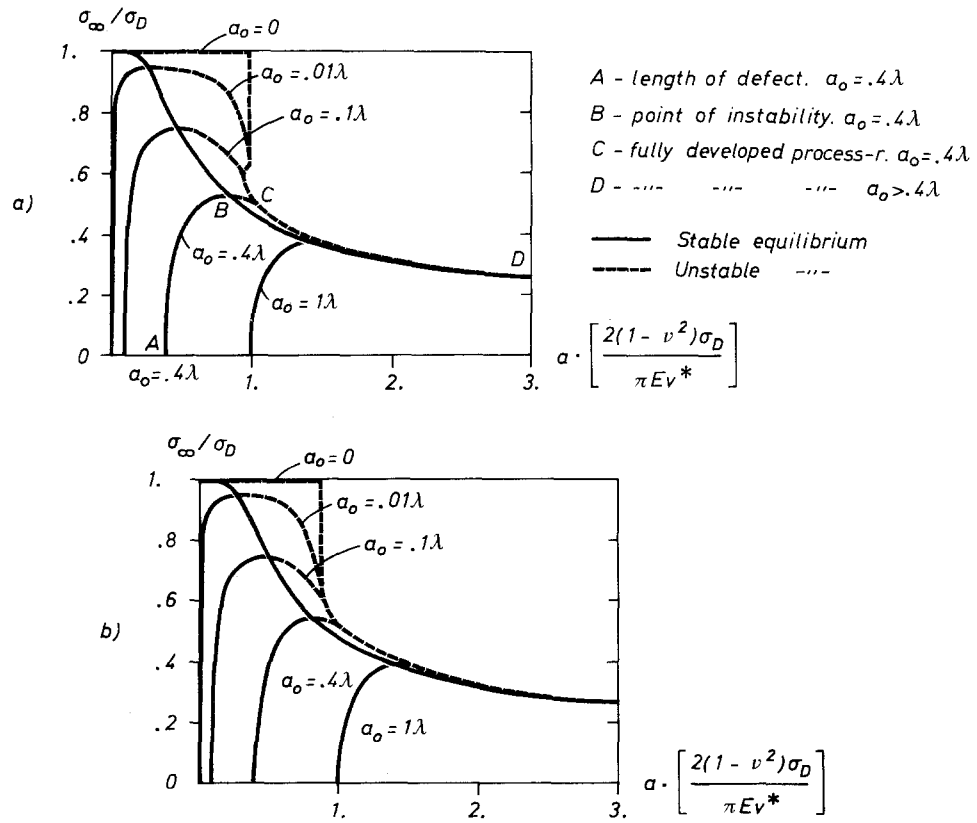

Figure 6. σ_∞ *vs.* total defect length $2a$. (a) model A and (b) model B. The path A–B–C–D in (a) describes the stable (A–B) and unstable (B–C–D) equilibrium of a crack developed from a slit of the length $2a_0 = .8\lambda$. $\lambda = \pi E v^*/(2(1 - \nu^2)\sigma_D)$.

of the region is

$$a - a_0 = g\pi E v^*/[2(1-\nu^2)\sigma_D]$$

$$\text{where } g = f(\beta)(1-\beta)/\beta \to \begin{cases} 1. & \text{when } a_0 \to 0 \\ .5 & \text{when } a_0 \to \infty \end{cases}$$

for model A. The numerical calculations of model B give

$$g \to \begin{cases} .87 & \text{when } a_0 \to 0 \\ .46 & \text{when } a_0 \to \infty. \end{cases}$$

Figure 8a and 8b illustrate the stress distribution at the process region for cracks of different lengths and their corresponding σ_{yy} *vs.* v relationships. The area under the graph $\sigma_{yy} = \sigma_{yy}(v)$ represents the amount of energy consumed in the fracture process, per produced unit surface area. According to the Griffith concept [4] this energy equals the elastic energy released at unit length crack growth and unit length thickness of the body, for a crack at equilibrium. Knowing the energy of the elastostatic field in the case of a point shaped process region, that is, when the crack length, $2a_0$, is large compared with the length of the process region, the appropriate remote stress is

$$\sigma_\infty = \left[\frac{2E\gamma}{\pi a_0(1-\nu^2)}\right]^{1/2}.$$

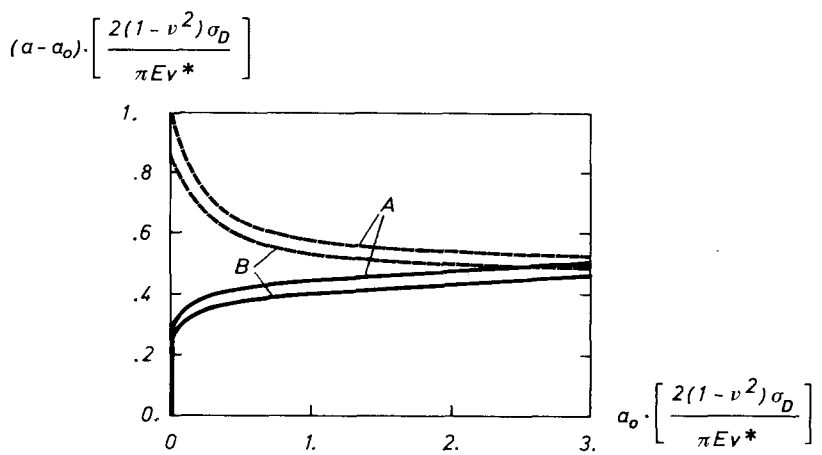

Figure 7. Length of the process region *vs.* crack length at the onset of instability and for the fully developed process region (dotted lines). The asymptotic values of $a - a_0$ at infinitly large cracks are .5 and .46 times $\pi E v^*/(2(1 - \nu^2)\sigma_D)$ for model A and B respectively.

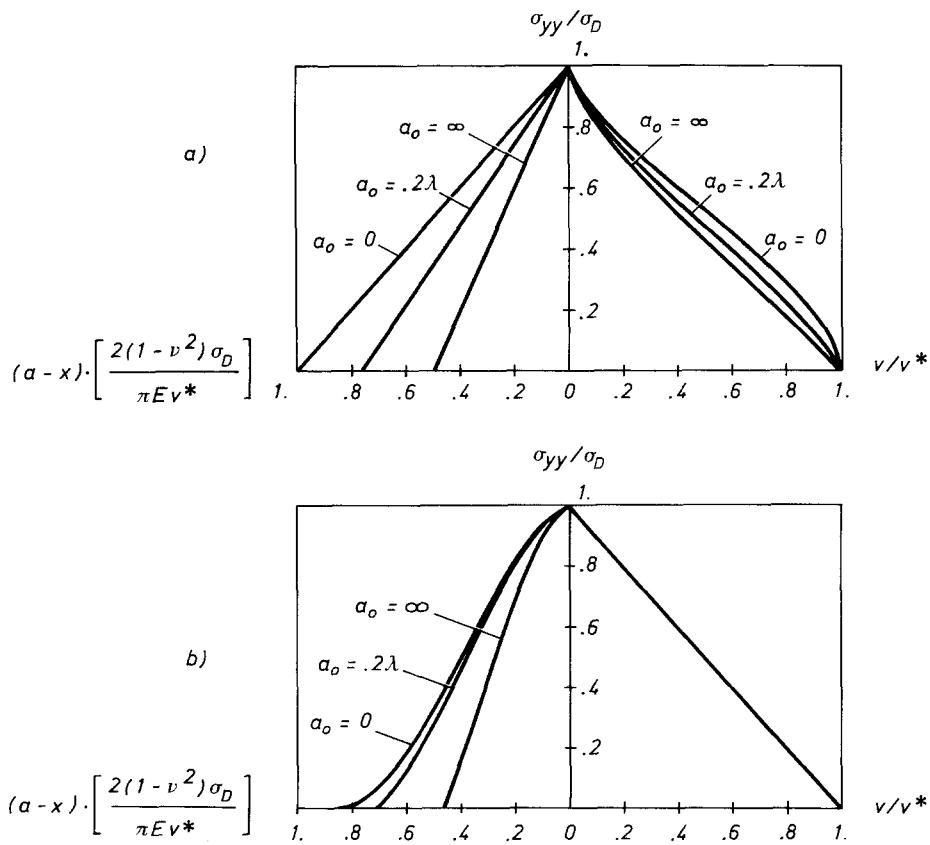

Figure 8. Cohesive stress σ_{yy} *vs.* distance $a - x$ from the crack tip and *vs.* discontinuous displacement in the process region. The figure displays the solution for a crack length $.2\lambda$ and the asymptotic solutions for an infinitly large crack and for a crack of zero length.

Here, using a line shaped process region, the asymptotic state of a large crack is examined. The remote stress in the case of an infinitely large crack is shown for model A (see appendix) and for different number of intervals, for model B. All results can be written on the form

$$\sigma_\infty = h\frac{E\sigma_D v^*}{\pi a_0(1-\nu^2)}$$

where h is a numerical factor, the value of which is given in the following table:

model	A	B($N=2$)	B($N=5$)	B($N=10$)
h	$(8/9)^{1/2} = .9428$	0.9871	0.9983	0.9997

As expected, the results show that the critical energy release rate is $2\gamma = 2\int_0^{v*} \sigma_{yy}\,dv$ in both model A and B. In model B this implies $2\gamma = \sigma_D v^*$ (since $h \to 1$ as $N \to \infty$) and in model A: $2\gamma = (8/9)\sigma_D v^*$. The appropriate σ_{yy} *vs.* v relationship for model A is shown by the curve $a_0 \to \infty$ in Fig. 8a.

Figure 9 shows the remote stress for small cracks when the process region is fully developed. However, this state is never reached under the condition of static equilibrium, since the maximum remote stress has occurred earlier. Thus, for instance, (13) gives

$$\sigma_\infty \to \sigma_D[1-(1-2/\pi)v_0/v^*] \quad \text{as} \quad a_0 \to 0$$

while the stress has dropped to $(2/\pi)\sigma_D$ when the process region is fully developed. Thus instability occurs when the remote stress reaches the value σ_D.

Instability. When very large bodies or load control are concerned, maximum remote stress is the significant fracture stress. At this stress the stable behaviour is replaced by unstable growth of the process region (i.e. increase of a) followed after some delay by unstable crackgrowth (i.e. increase of a_0).

Figure 7 shows the length of the process region at onset of instability. For model A the equation $d\sigma_\infty/d\beta = 0$ has been used. This is equal to $d\sigma_\infty/da = 0$ since the crack length a_0 is

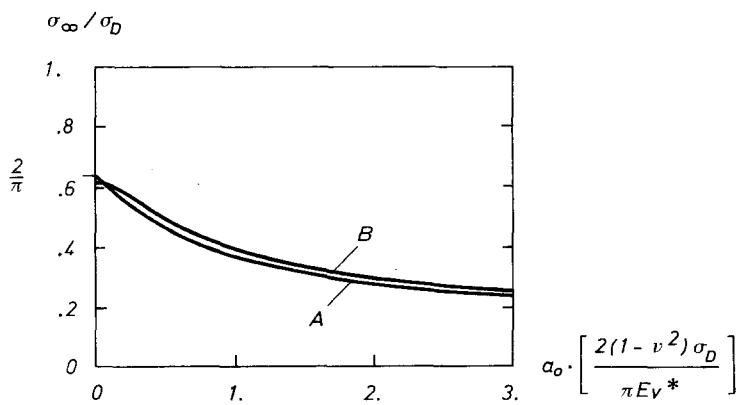

Figure 9. Remotely applied stress σ_∞ *vs.* crack length $2a_0$, when the process region is fully developed. Note that this stress is not necessarily equal to the maximum remote stress.

constant at onset of instability and $\beta = a_0/a$. Together with (13) and (14) this gives the value of β and thus the length of the process region. Note that $d\alpha/d\beta = \alpha/\beta$. It is observed (see Fig. 7) that the length of the process region approaches zero for small cracks. In fact it can be shown that $a - a_0 \approx a \sim [\ln(\text{const.}/a_0]^{-1/2}$ as $a_0 \to 0$.

Models A and B differ only slightly as regards prediction of the critical remote stress $\sigma_{\infty c}$ at onset of instability as a function of the crack length. Thus assuming the two models to give the same prediction for very large cracks the maximum deviation, which occurs for vanishingly small crack length, is only a few per cent, see Fig. 10. The figure also show the relative difference in predictions by conventional large crack fracture mechanics and model B. Also here the two predictions are assumed to coincide for very large cracks. The prediction

$$\sigma_{\infty c} = K_{Ic}(\pi a_0)^{1/2}$$

by conventional fracture mechanics gives the relation between $\sigma_{\infty c}$ and the non-dimensional crack length in Fig. 10 after recognizing that

$$K_{Ic} = [2\gamma E/(1 - \nu^2]^{1/2} = [\sigma_D v^* E/(1 - \nu^2]^{1/2}.$$

The ASTM convention of linear fracture mechanics can be written

$$a_0[2(1 - \nu^2)\sigma_D/\pi E v^*] \geqslant 5/\pi.$$

As can be seen from Fig. 10 this implies less than about 5% difference in the prediction of $\sigma_{\infty c}$ between conventional large crack fracture mechanics and model B. An attempt to extend the validity of conventional large crack fracture mechanics to smaller crack lengths would result in increasing differences with decreasing crack length. Thus the remote stress $\sigma_{\infty c}$ predicted would be about 50 per cent higher if conventional large crack fracture mechanics were used instead of model B (or model A) for a crack length that is about one tenth of the minimum length allowed by the ASTM convention.

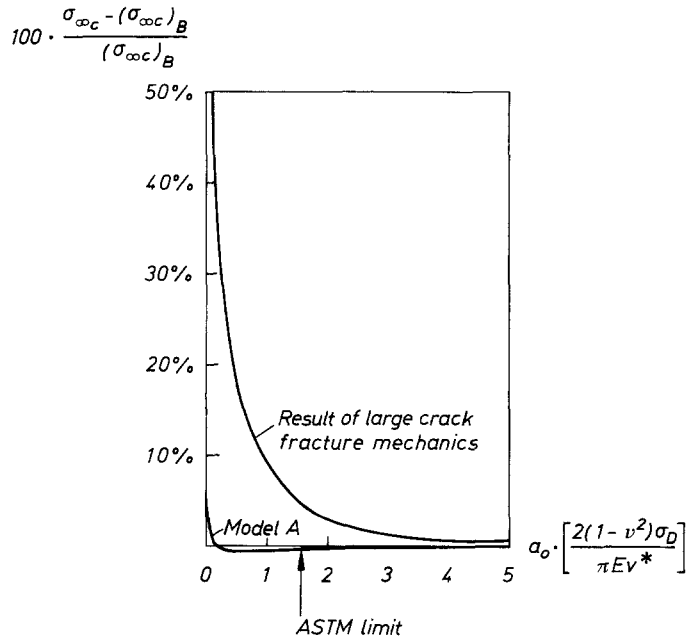

Figure 10. The relative difference in maximum remote stress $\sigma_{\infty c}$ as predicted by (1) large crack fracture mechanics and model B and (2) model A and model B.

For large cracks onset of instability and fully developed process region coincide, and, as has been seen, the models are in agreement with the Griffith model [4], since it predicts instability when the elastic energy released from the stress-strain field equals the energy required to produce fracture surfaces.

Acknowledgements

For general encouragement and many valuable discussions during the work, my thanks are due to Dr. H. Andersson and for critical comments on the manuscript also to Prof. B. Broberg.

REFERENCES

[1] W.F. Brown and J.E. Srawley, Plane Strain Crack Toughness Testing of High Strength Metallic Materials, ASTM Special Technical Publication 410 (1966).
[2] G.I. Barenblatt, *Advances in Applied Mechanics* 7 (1962) 55–129.
[3] N.I. Muskhelishvili, *Some Basic Problems of the Mathematical Theory of Elasticity*, P. Noordhoff Ltd., Groningen, Holland (1953).
[4] A.A. Griffith, *Philosophical Transactions of the Royal Society* (London) A221 (1920) 163–198.
[5] D.S. Dugdale, *Journal of the Mechanics and Physics of Solids* 8 (1960) 100–104.
[6] B.A. Bilby, A.H. Cottrell and K.H. Swinden, *Proceedings of the Royal Society* (London) A272 (1963) 304–314.
[7] J.R. Rice, *Fracture II*, Academic Press, New York (1968) 191–311.

Appendix

Dugdale [5] gave the length $a - a_0$ of a strip shaped plastic zone with a constant cohesive stress σ_D through the relation

$$a_0/a = \cos\left(\frac{\pi}{2}\frac{\sigma_\infty}{\sigma_D}\right)$$

The relation is obtained identically from (13) if v_0 is equal to zero.

Later Bilby, Cottrell and Swinden [6] derived expressions for the displacement at the process region which are in agreement with (12) if v_0 is put to zero.

To obtain solutions for large cracks in the case of the approximate model A, let $a_0\sigma_D^2/K_{Ic}^2$ tend to infinity. With coordinates according to Fig. A1 the stress at the process region transforms to

$$\sigma(\xi) = \sigma_D(1 + (\xi - 1)v_0/v^*) \tag{A1}$$

and the dimensionless displacement is found from (12)

$$v(\xi)/v^* = (2\delta/\alpha)\{(1-\xi)^{1/2} - \xi\tanh^{-1}[(1-\xi)^{1/2}] + \\ + (v_0/v^*)(\xi/2)[(2-\xi)\tanh^{-1}[(1-\xi)^{1/2}] - (1-\xi)^{1/2}]\} \tag{A2}$$

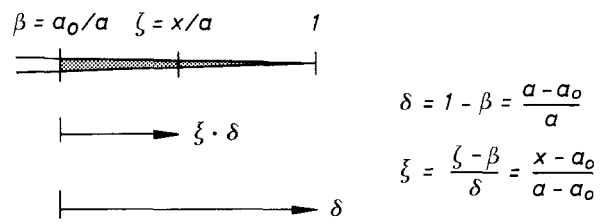

Figure A1. Dimensionless coordinates.

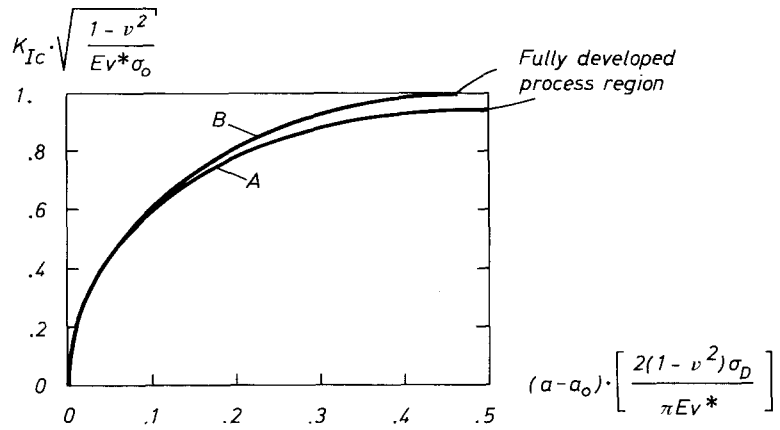

Figure A2. Stress intensity factor *vs.* length of the process region for an infinitely large crack.

where $\alpha = \pi E v^*/[2a(1-\nu^2)\sigma_D]$.

The crack opening displacement can be calculated from the expression

$$v_0 = \lim_{\xi \to 0} v(\xi)$$

The result

$$v_0/v^* = 2\delta/\alpha \tag{A3}$$

can be used together with (A2) to give

$$v(\xi)/v^* = (2\delta/\alpha)\{(1-\xi\delta/\alpha)(1-\xi)^{1/2} - [1-(2-\xi)\delta/\alpha]\xi \tanh^{-1}[(1-\xi)^{1/2}]\}. \tag{A4}$$

When a body containing a crack with an infinitesimally small process region is subject to small loads $v_0 \ll v^*$ and as a consequence of (A1) we have a Dugdale model. According to (A2)

$$v(\xi)/v^* = (2\delta/\alpha)\{(1-\xi)^{1/2} - \xi \tanh^{-1}[(1-\xi)^{1/2}]\}$$

which is equal to the displacement in the cohesive zone given by Rice [7].

Each value of the load parameter $K_I = \sigma_\infty(\pi a_0)^{1/2}$ below K_{Ic} corresponds, for a fixed crack length $2a_0$, to a certain length, $a - a_0$, of the process region. From (13) and (A3) it is found

$$K_I = 2\sigma_D[1-(2/3)(\delta/\alpha)](2a\delta/\pi)^{1/2}.$$

Maximum of K_I is found for $\delta = \alpha/2$ which implies $a - a_0 = \pi E v^*/[4(1-\nu^2)\sigma_D]$ (see Fig. A2). With the present boundary conditions this would correspond to onset of crack growth, i.e. a growing a_0. This means that the crack grows when

$$K_I = (2/3)(2Ev^*\sigma_D/(1-\nu^2)]^{1/2}$$

which is consistent with the fact that $2\gamma = (8/9)\sigma_D v^*$ for model A. When $\delta = \alpha/2$ it is also found from (A3) that $v_0 = v^*$. So, unlike the short crack (c.f. Fig. 6) the large crack grows at the instant the process region is fully developed.

A numerical investigation of the B model makes it possible to plot K_I as the process

region develops (see Fig. A2). Maximum remotely applied load is found when the process region has grown to the length $a - a_0 = .46\pi Ev^*/[2(1 - \nu^2)\sigma_D]$ giving

$$K_I = [Ev^*\sigma_D/(1 - \nu^2)]^{1/2}$$

as it should, since here the "surface energy" $2\gamma = \sigma_D v^*$.

RÉSUMÉ

La limite de validité de la mécanique de rupture linéaire est déterminée par la longueur de fissure minimale permise, selon une convention adoptée par l'ASTM. Une extension dans des régions non linéaires devrait impliquer une extension vers des fissures admissibles de plus petites longueurs. Une étude pilote a été entreprise en vue d'élucider la question suivante: quelle est la plus courte fissure à laquelle s'applique la méthode de mécanique de rupture et comment se comportent les fissures plus courtes que celle-là?. On a modélisé une région de travail comme une région linéique de Barenblatt et on a négligé les écoulements plastiques hors de la région de travail. Les résultats montrent qu'une instabilité se produit avant que ne se développe complètement la région de travail (ainsi que c'est le cas pour des grandes fissures) si la fissure est courte. Ceci implique de grandes déviations par rapport à la mécanique de rupture applicable aux fissures larges, si la fissure est très petite. On inclut même dans l'étude le cas de fissures de longueur infinitésimales.